Electronic Supplementary Material (ESI) for Inorganic Chemistry Frontiers.

Supplementary Information

Bimetal-doped cobalt oxyhydroxides/hydroxides synthesized by electrochemistry for enhanced OER activity

Rongmei Zhu,*[a] Yi Zhang,[a] Limei Liu,[a] Yong Li,[a] Gaihua He,[b] and Huan Pang*[a]

School of Chemistry and Chemical Engineering, Institute for Innovative Materials and Energy, Yangzhou University, Yangzhou, 225009, Jiangsu, P. R. China

*Corresponding authors: rmzhu@yzu.edu.cn (R. Zhu), huanpangchem@hotmail.com, panghuan@yzu.edu.cn (H. Pang)

Table of Contents

Chemical reagents and materials

Cobalt(II) nitrate hexahydrate ($Co(NO_3)_2 \cdot 6H_2O$, 98%), 2-methylimidazole ($C_4H_6N_2$, 2-MeIM, 99%) , potassium hydroxide (KOH, 85%), purchased from Aladdin Reagents and used as received. Hafnium(IV) chloride ($HfCl_4$, ≥98%), Ammonium iron(III) sulfate ($NH_4Fe(SO_4)_2$, ≥98%), Carbon paper was purchased from Hesen corporation.

Pre-treatment of carbon paper

The native carbon paper was placed in furnace and calcined at 500 ℃ for 4 h in atmosphere.

Synthesis of Co-MOF

1 mmol (0.291 g) of cobalt nitrate hexahydrate were dissolved in 25 mL of deionized water and noted Solution A. 2.5 mmol (0.2052 g) of 2-methylimidazole were dissolved in 25 mL of deionized water and noted Solution B. The carbon paper was placed in solution A and soaked with stirring for 2 h. Then solution B was poured into solution A, and mixed solution and carbon paper were transferred to the liner of the PTFE reactor. The reactor was sealed and transferred to an oven at 160 °C for 8 h. The carbon paper was washed with methanol after reaction. Finally, the Co-MOF-loaded carbon paper was dried in an oven at 60 °C overnight.

Synthesis of (Hf)CoOOH/$Co(OH)_2$

Certain amount of $HfCl_4$ was added to a solution of 0.1 M KOH. Then carbon paper loaded with Co-MOF was placed in the mixed solution. Electrochemical cyclic voltammetry was used for the etching at this condition. The voltage range was set to 0-0.6 V (vs Hg/HgO) with a sweep rate of 10 mV s^{-1}. Then, the carbon paper was collected after a certain number of cycles until the Co-MOF was gradually transformed into green, and washed with deionized water.

Synthesis of (Fe,Hf)CoOOH/$Co(OH)_2$

Carbon paper loaded with (Hf)CoOOH/$Co(OH)_2$ was placed in an aqueous solution of 0.15 M ammonium iron sulfate. Electrosorption Fe^{3+} for 1150 s at a current density of 1 mA cm^{-2} using chronopotentiometry. The high potential limit of chronopotentiometry is need to set an unreachable value, which was 4 V in this experiment.

Synthesis of CoOOH/$Co(OH)_2$

Synthesize procedure is consistent with (Hf)CoOOH/$Co(OH)_2$, but do not add $HfCl_4$ to the KOH solution.

Synthesis of (Fe)CoOOH/$Co(OH)_2$

Synthesize procedure is same as (Hf)CoOOH/$Co(OH)_2$, but do not add $HfCl_4$ to the KOH solution. The process of electrosorption of Fe^{3+} is consistent with the conversion of (Hf)CoOOH/$Co(OH)_2$ to (Fe,Hf)CoOOH/$Co(OH)_2$ except using carbon paper loaded with CoOOH/$Co(OH)_2$.

Characterization

Scanning electron microscopy (SEM) images were obtained on a Zeiss Supra55 microscope. The samples were tested by X-ray diffraction (XRD) on a Rigaku-Ultima III with Cu Kα radiation (λ = 1.5418 Å) for the phase analysis. High-resolution transmission electron microscopy (HRTEM) images and SAED images were captured on a Tecnai G2 F30 transmission electron microscopy at an acceleration voltage of 300 kV. X-ray photoelectron spectroscopy (XPS) analysis was carried out using a Thermo Scientific ESCALAB 250Xi X-ray photoelectron spectrometer.

Electrochemical measurements

All the electrochemical measurements were carried out in a three-electrode system via a CHI-760E (Shanghai Chenhua) instrument at room temperature. A Carbon paper loaded with catalyst was employed as the working electrode, graphite carbon rod as counter electrode, and Hg/HgO electrode as reference electrode in 1.0 M KOH electrolyte. Linear sweep voltammetry curves were measured at a sweep rate of 5 mV s^{-1}. The sample loading is 0.35 mg/cm^{-2}. The measured potentials of all the data were converted to RHE scale according to the Nernst equation ($E_{RHE} = E_{Hg/HgO} + 0.059 \times pH + 0.098$) scale.

Electrochemical calculation

Through adjusting to the Tafel equation ($\eta = b \log j + a$, where η is the overpotential, b is the Tafel slope, j is the current density and a is the exchange current density), the Tafel slopes and exchange current densities could be calculated for prepared materials.

DFT Calculations

The density functional theory (DFT) calculations were implemented by the Vienna Ab initio Simulation Package (VASP). The ion-electron interaction was described according to the projector augmented wave (PAW). The exchange–correlation functional was adopted in the generalized gradient approximation (GGA) using Perdew-Burke-Ernzerhof (PBE) method. The kinetic cutoff energy was chosen at 400 eV, and the changes in total energies and the atomic force were set to be 10^{-4} eV and 0.02 eV/Å, respectively. For the structure optimizations, a 2×2×1 Monkhorst–Pack (MP) kpoint grid was utilized.

The difference in the number of electrons with opposite spin directions on the Fermi surface was calculated through spin polarization analysis. The specific rules are as follows:

$$\text{Spin polarization} = \left| \frac{e_{\uparrow} - e_{\downarrow}}{e_{\uparrow} + e_{\downarrow}} \right|$$

where $e_{\uparrow}$ and $e_{\downarrow}$ represent the charge density of spin-up and spin-down electrons, respectively, in the real space with an energy interval of [ε, E_f]. In this work, the energy range of [E_f-0.2 eV, E_f] was used. To estimate the OER catalytic activities of (Fe)CoOOH/$Co(OH)_2$ and (Fe,Hf)CoOOH/$Co(OH)_2$, we computed the Gibbs free energy (ΔG) of each reaction step in OER. On the basis of this model, the ΔG of each elementary step can be determined by:

$* + OH^- \rightarrow *OH + e^- \Delta G_1$

$*OH + OH^- \rightarrow *O + H_2O + e^- \Delta G_2$

$*O + OH^- \rightarrow *OOH + e^- \Delta G_3$

$*OOH + OH^- \rightarrow * + O_2 + H_2O + e^- \Delta G_4$

$\Delta G = \Delta E + \Delta ZPE - T\Delta S$, where ΔE can be directly determined from DFT computations. ΔZPE refers to the change in zero-point energy, while ΔS denotes the energy difference of entropy, and T is the room temperature (298.15 K). Notably, the ZPE and S of oxygenated intermediates

in OER were obtained by computing their vibrational frequencies, while those of free H_2 and H_2O molecules were obtained from the NIST database. The potential of (H^++ e^-) in solution at standard conditions was assumed as the potential of 1/2 H_2. The Gibbs free energy of O_2(G_{O2}) was determined according to the following equation: $G_{O2}=G_{H2O}-2G_{H2}+4.92eV$. After obtaining the ΔG values of each elementary step in OER, the limiting potential (U_L) an be obtained: $U_L=\max(\Delta G_1, \Delta G_2, \Delta G_3, \Delta G_4)/e$, which has been widely-accepted as the descriptor for thermodynamically evaluating the catalytic performance of OER on a given electrocatalyst.

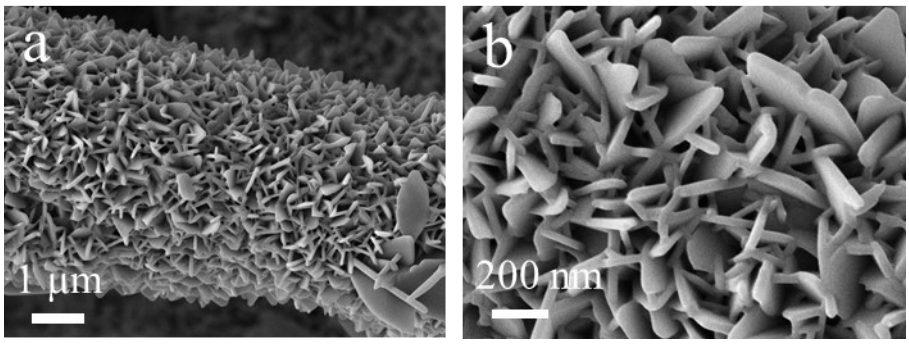

Figure S1. (a)Low and (b) high magnificent SEM images of Co-MOF.

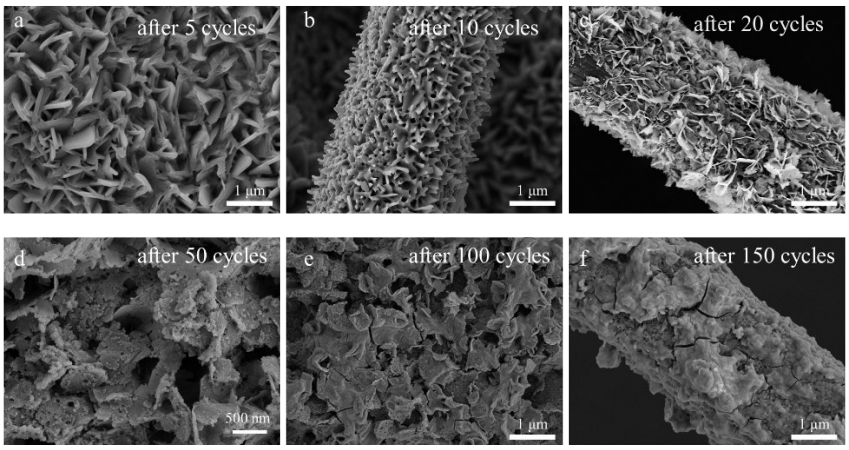

Figure S2. SEM images of electrochemical Lewis acid co-etched samples with (a)5, (b)10, (c)20, (d)50, (e)100, (f)150 cycles of CV.

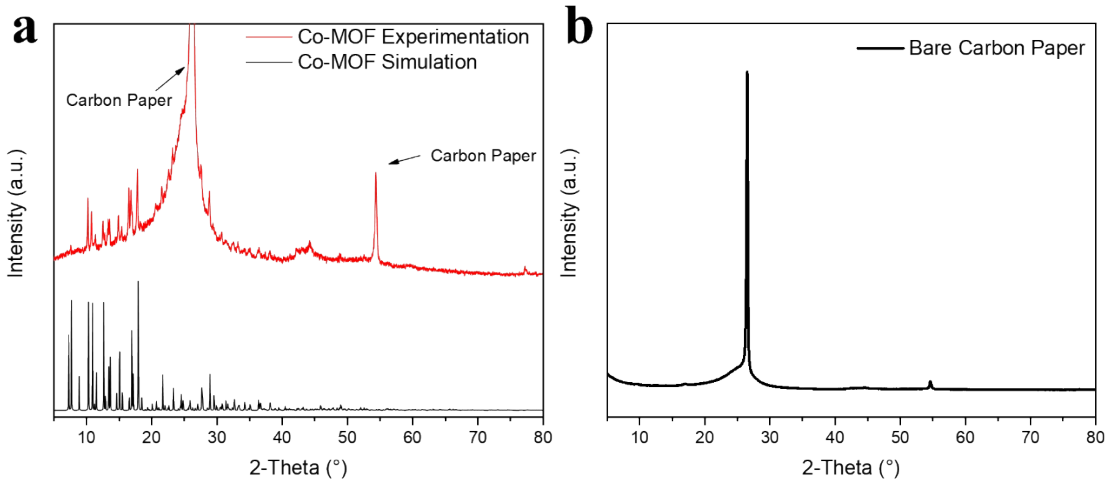

Figure S3. (a) Experimental and simulated XRD patterns of Co-MOF; (b) XRD pattern of bare carbon paper.

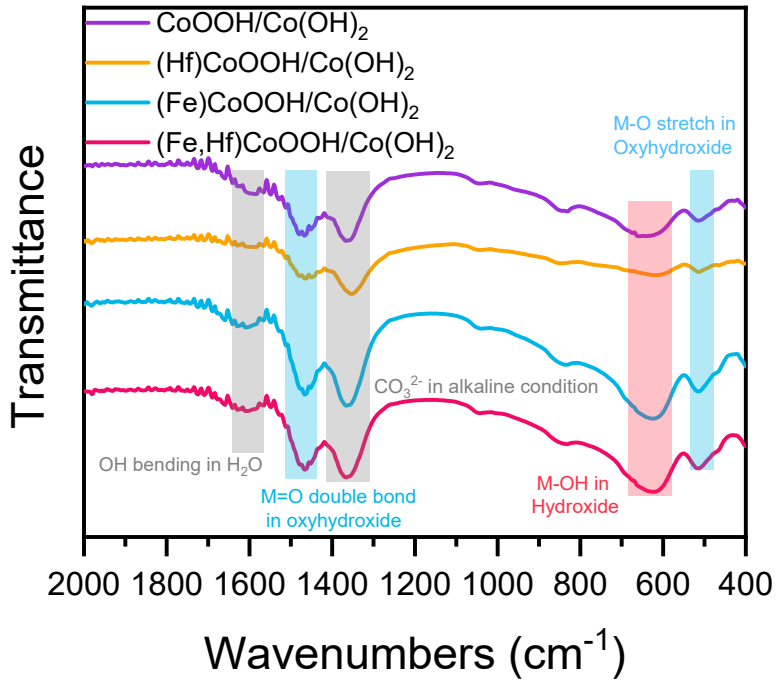

Figure S4. FT-IR patterns of $CoOOH/Co(OH)_2$, $(Hf)CoOOH/Co(OH)_2$, $(Fe)CoOOH/Co(OH)_2$, and $(Fe,Hf)CoOOH/Co(OH)_2$.

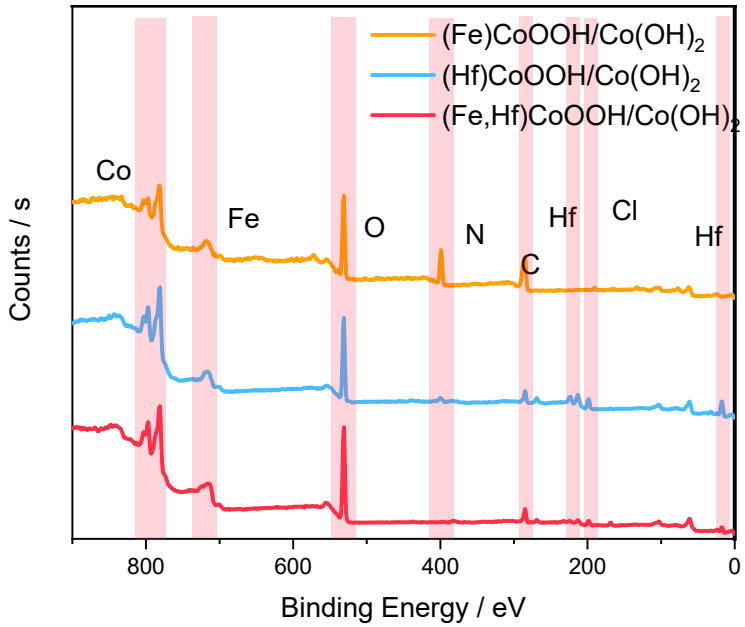

Figure S5. Survey XPS spectra of (Fe)CoOOH/$Co(OH)_2$, (Hf)CoOOH/$Co(OH)_2$, and (Fe,Hf)CoOOH/$Co(OH)_2$.

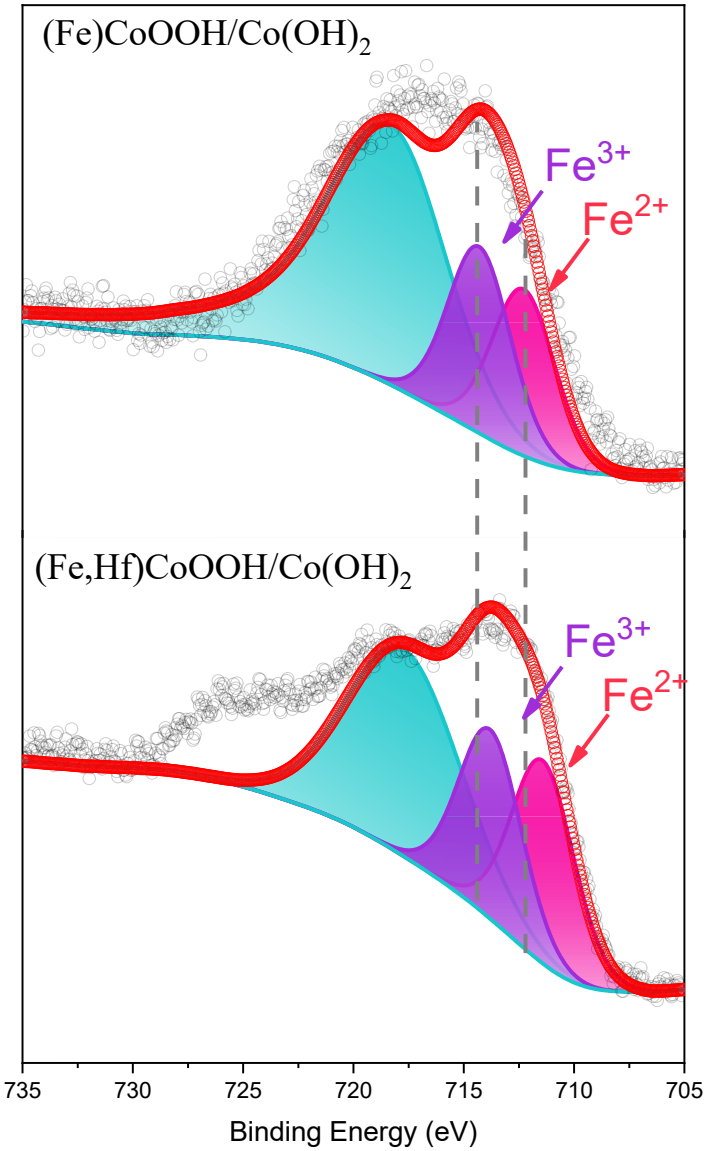

Figure S6. High-resolution XPS spectra of Fe 2p in the samples of (Fe)CoOOH/$Co(OH)_2$ and (Fe,Hf)CoOOH/$Co(OH)_2$.

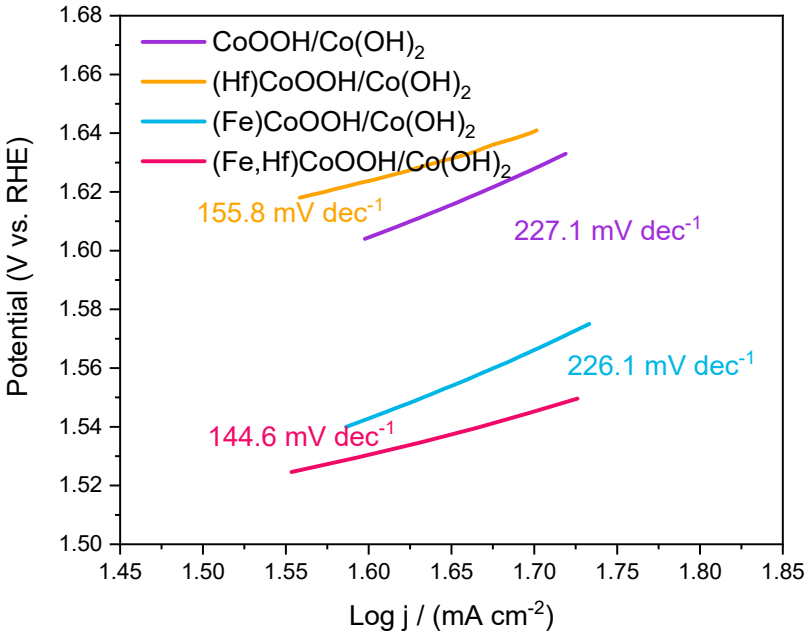

Figure S7. Tafel slop plot of all four catalysts at high potential.

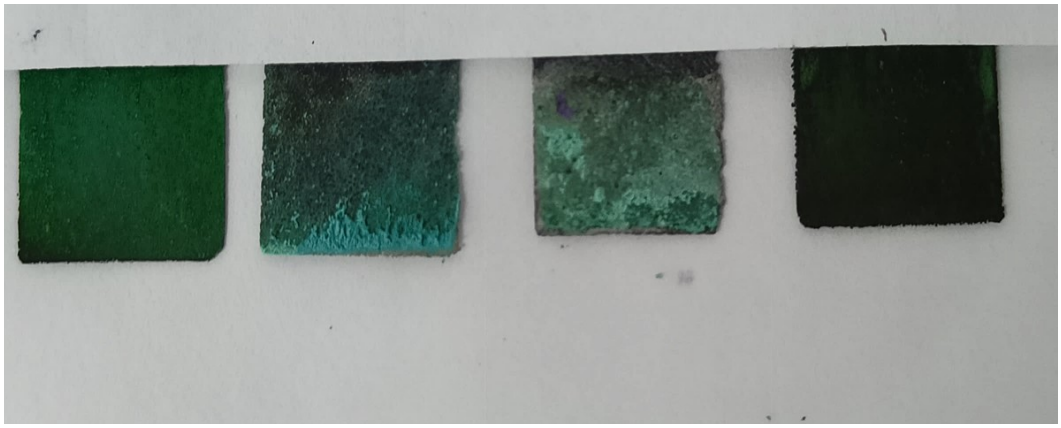

Figure S8. The optical photo of $CoOOH/Co(OH)_2$, $(Hf)CoOOH/Co(OH)_2$-0.75, $(Hf)CoOOH/Co(OH)_2$-1.5, and $(Hf)CoOOH/Co(OH)_2$-2.25 (from left to right respectively).

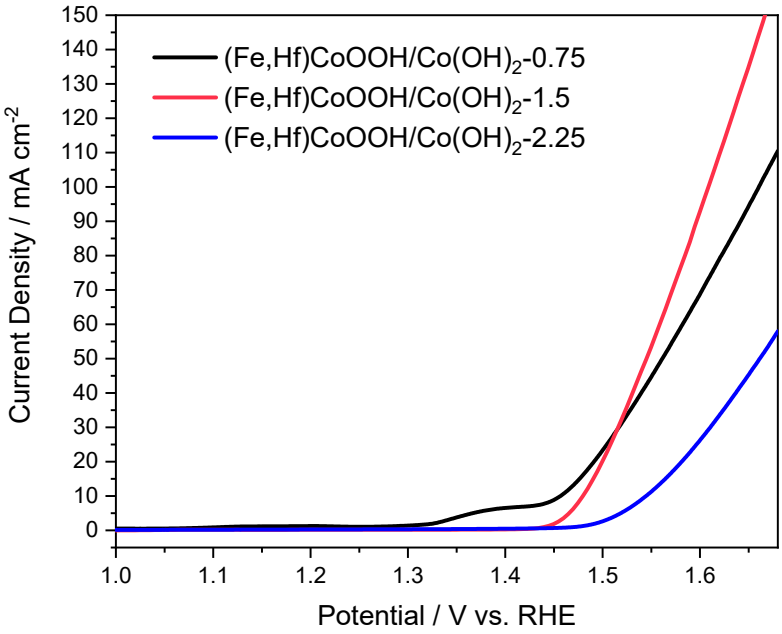

Figure S9. LSV plots of (Fe,Hf)CoOOH/$Co(OH)_2$ with different Hf^{4+} dosages.

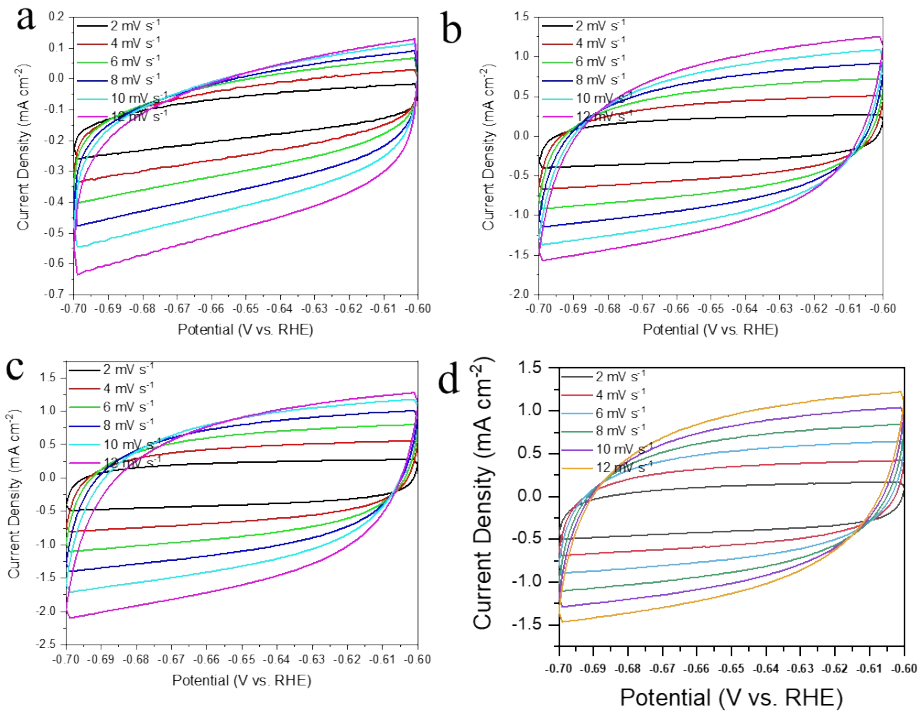

Figure S10. The CV curves from -0.7 to -0.6 V vs RHE of (a)$CoOOH/Co(OH)_2$, (b)$(Hf)CoOOH/Co(OH)_2$, (c)$(Fe)CoOOH/Co(OH)_2$, and (d)$(Fe,Hf)CoOOH/Co(OH)_2$

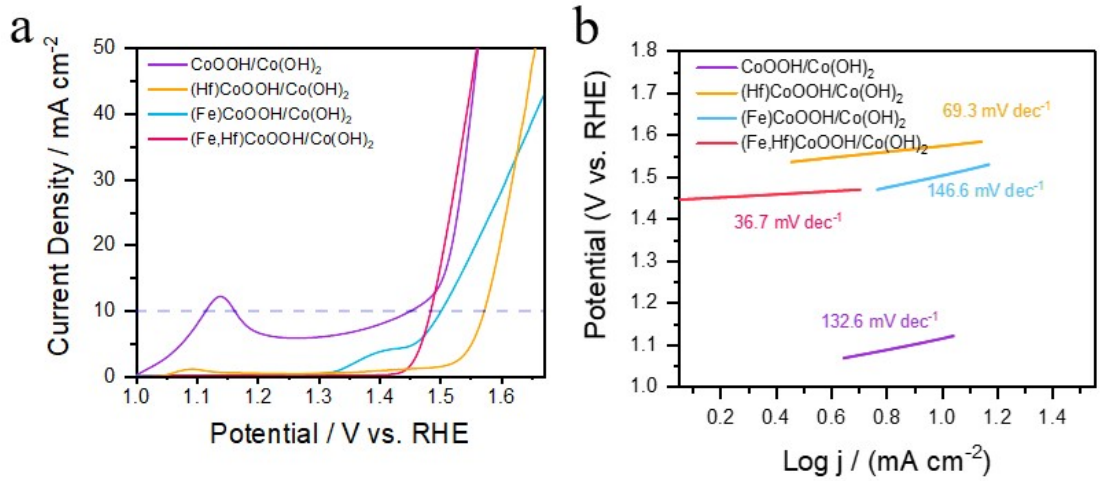

Figure S11. (a)Normalized LSV polarization curves and (b)corresponding Tafel slopes.

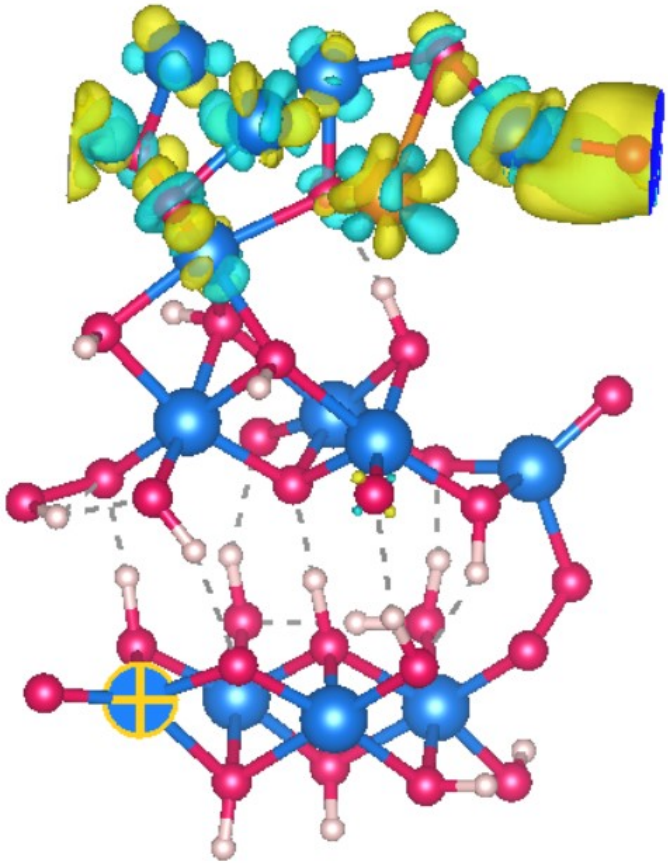

Figure S12. The differential charge densities of (Fe)CoOOH/$Co(OH)_2$ with O*.

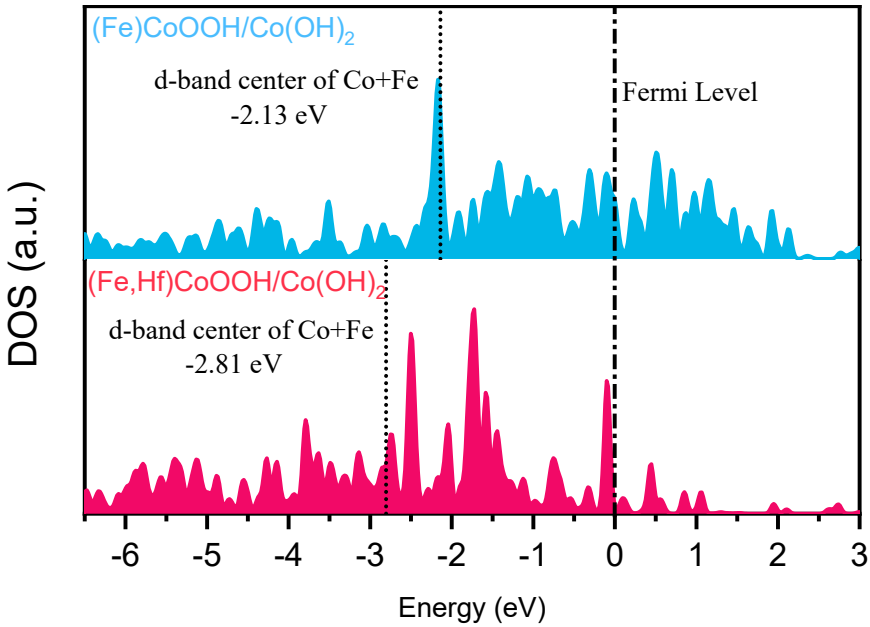

Figure S13. PDOS plots of Co+Fe sites in (Fe,Hf)CoOOH/$Co(OH)_2$ and (Fe)CoOOH/$Co(OH)_2$.

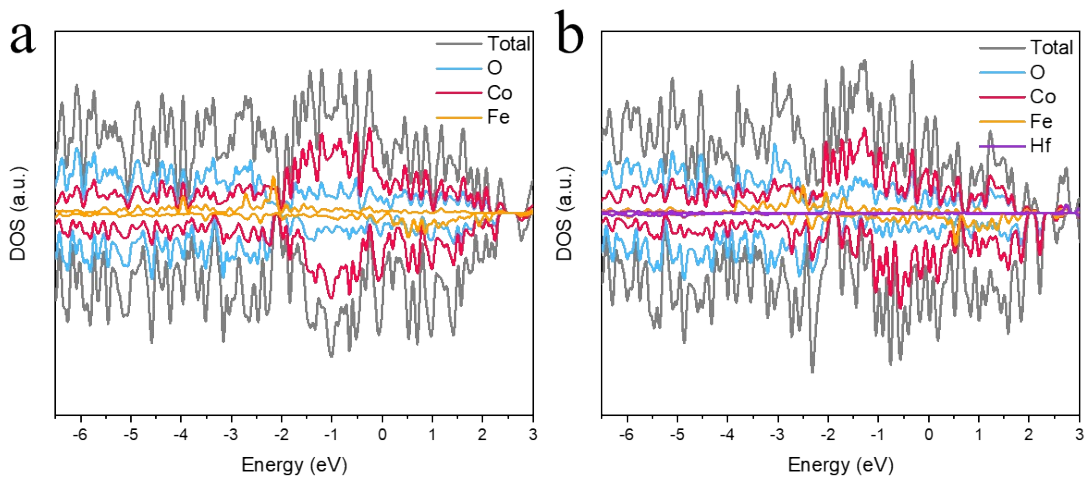

Figure S14. The projected density of states on (a) (Fe)CoOOH/$Co(OH)_2$ and (b) (Fe,Hf)CoOOH/$Co(OH)_2$ model.

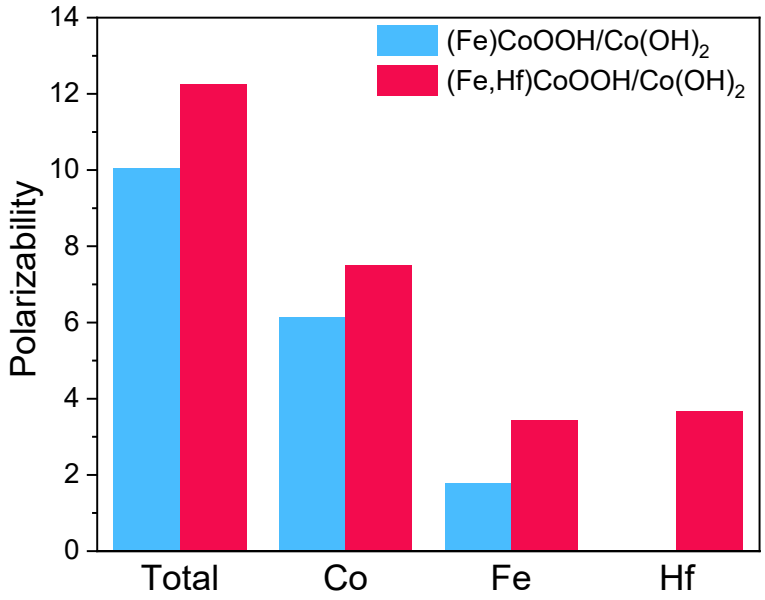

Figure S15. Spin polarizability of (Fe)CoOOH/$Co(OH)_2$ and (Fe,Hf)CoOOH/$Co(OH)_2$ (calculated with the energy interval of [E_f-0.2 eV, E_f]).

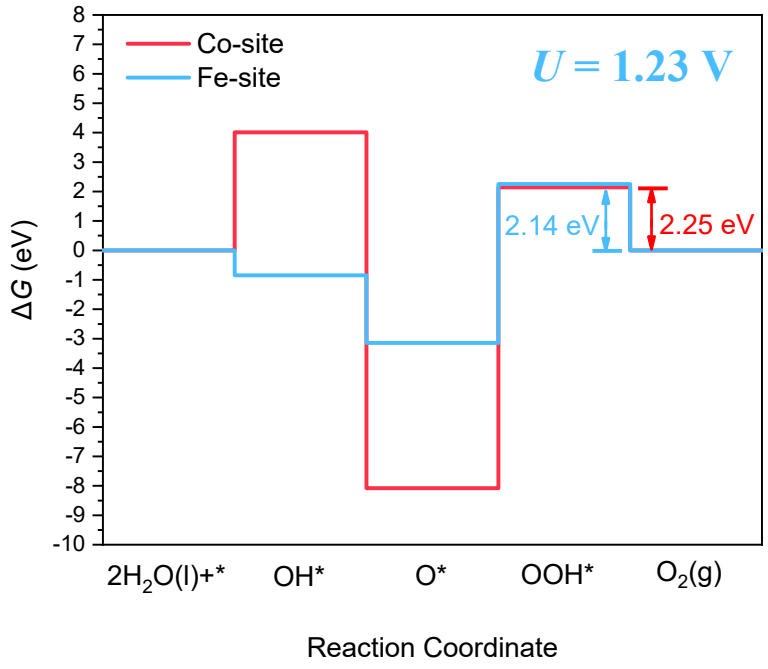

Figure S16. Gibbs free energy diagrams for (Fe)CoOOH/$Co(OH)_2$ at U=1.23 V.

Table S1. Comparisons of OER performance for various electrocatalysts in 1.0 M KOH from other publications.

Catalysts	Overpotential at 10 mA cm^{-2} [mV]	Tafel slop [mV dec^{-1}]	Ref.
(Hf,Fe)OOH/$Co(OH)_2$	250	37.6	This work
Co_3Mo/Mo_2C@NC	282	59.3	*Adv. Funct. Mater*. 2024, 34, 2314247
Co-Mo-N-PHP	294	57	*Appl. Catal. B: Environ.*, 2019, 255, 117744
P-NiO/$NiCo_2O_4$	290	49.6	*J. Alloys Compd*. 2022, 925, 166338
FeOOH−$CoMoO_4$	298	80.7	*ACS Appl. Mater. Inter.* 2021, 13, 17450−17458
CoFe-P	293	—	*Adv. Energy Mater.* 2022, 12, 2201141
$Li_{0.5}Zn_{0.5}Fe_{0.125}Co_{1.875}O_4$	350	—	*Angew. Chem. Int.* Ed. 2019, 58, 6042-6047
γ-MnOOH/CoOOH	313	87	*Chem Commun,* 2020, 56, 15387
CoP@CoOOH/CP	331	148	*Small* 2022, 18, e2106012
CoCu@HNC	289	131.8	*CCS Chem.* 2024, 6, 1324–1337
H-SCP	291	38	*J. Colloid Interface Sci.*2023, 631,8-16
Co_3O_4/Co-Fe	297	61	*Adv. Mater.* 2018, 30, 1801211
FeCoNi-LDH	269	42.3	*Adv. Energy Mater*. 2021, 11, 2102141
Fe-Co_xP	300	49	*Chem. Eng. J,* .2021, 409, 128227
(Fe,Co)OOH/MI	230	73	*Adv. Mater.* 2022, 34, 2200270